Structural, electric and magnetic properties of Ce-substituted Ni-Cu-Zn ferrite

A M Shahare
Department of Physics,
Dhote Bandhu Science College, Gondia, India
Email- amshahare@gmail.com

D S Choudhary
Department of Physics,
Dhote Bandhu Science College, Gondia, India
Email- dschoudhary@dbscience.org

A V Bagde
Department of physics
Chintamani Science College, Pombhurna,
Chandrapur-441224, Maharashtra, India
Email:akashbagde24@rediffmail.com

A S Nagpure
Department of Applied Physics,
MIET, Kudwa, Gondia, 441614, India
Email: anu.balaghat@gmail.com

Abstract- The effect of Ce substitution on structural, magnetic and electric properties of Ni-Cu-Zn ferrite of chemical formula $Ni_{0.25}Cu_{0.2}Zn_{0.55}Fe_{2-x}Ce_xO_4$ (x=0.0 to x=0.25 with step 0.05) which prepared by nitrate-citrate sol gel auto combustion method has been studied. To characterize the properties of the samples X-ray diffractometer (XRD), Scanning electron microscopy (SEM), Vibrating sample magnetometer (VSM), impedance analyzer have been practiced. The XRD study confirms the cubic spinel structure along with single phase. It is inferred now crystalline size decreases while X-ray density and porosity increases with Ce content in samples. SEM micrograph mirrors that the average grain size is dimished with increasing Ce-content. Decrease in Saturation magnetization (M_s), Remanent magnetization (M_r) and increase in Coercivity (H_c) have been observed in Cerium doped ferrite samples. Changes in dielectric constant, dielectric loss ($tan\ \delta$) and AC conductivity are observed as a function of frequency and Ce concentration. AC Conductivity is found to increase with the Ce content. The dielectric loss of Ce doped samples is found higher than the un-doped sample.

Keywords – Spinel Ferrite, XRD, SEM, Magnetic properties, electrical properties.

I. INTRODUCTION

The fascinating magnetic and electric properties of ferrites make them commercially significant in wide range of applications like electronic, magnetic, electrochemical and microwave devices, in power generation, conditioning and conversion [1,2]. In particular, the spinel structure Ni-Cu-Zn ferrites have wide potential for multilayer chips inductor (MLCI and high frequency applications due to their low electrical conductivity, high permeability and low sintering temperature [3-7]. MLCIs are also extensively applied in many electronic devices and they have greatly assisted miniaturization of the many of the latest electronic products, including the present electronic appliances available for the mankind. The magnetic properties pertaining to the concerned ferrites are affected by their chemical composition,

presence of small additives and microstructures i.e. grain size, porosity and specially grain boundary characteristics like elastic strain field [8-10]. Dissimilar compositions of ferrites in powder form with low sintering temperature are being widely studied in these years. The investigation on La-substituted Ni-Cu-Zn ferrite [11] has given promising result from the technological point of view, with a significant increase upto an extent in relative permeability compared with un-substituted ferrites and then decreases. Also, the composition $Ni_{0.25}Cu_{0.2}Zn_{0.55}Fe_{1.95}Sm_{0.05}O_4$ shows significant electromagnetic properties is as well as it proved to be the most useful material for MLCI applications Fe^{2+} ions are predicated to be at least in Sm-substituted ferrites because of the constitution of secondary phase $SmFeO_3$ which disallow the oxidation of Fe^{3+} inside the grains. For $CuFe_{2-x}Pr_xO_4$ (x = 0.0 to 0.1) no secondary phase is observed however the ionic radius of Pr^{3+} (1.013 Å) is higher than the ionic radius of Fe^{3+} (0.67 Å) and the replacement at tetrahedral sites is very occasional [12]. In addition to this, various researchers have studied different compositions for different substitutions and their studies provide significant enhancement in the electric and magnetic properties. Based on partial substitution of diatomic and triatomic cations in Ni-Cu-Zn ferrites, the present work is devoted to find out the effect of Ce substitution on micro-structure, densification and electromagnetic properties of $Ni_{0.25}Cu_{0.2}Zn_{0.55}Fe_{2-x}O_4$ with the steps of 0.905 (0.00-0.25) nano crystalline ferrite prepared by combustion method and studied for structural, electric and magnetic properties.

II. EXPERIMENTAL PROCEDURE

2.1 Ferrite synthesis and characterization–

Mixed Ni-Cu-Zn ferrites having chemical formula $Ni_{0.25}Cu_{0.2}Zn_{0.55}Fe_{2-x}Ce_xO_4$ with x=0.00 to 0.25 are synthesized by sol-gel auto combustion technique. All chemicals used are of analytical grade. Nickel nitrate [$Ni(NO_3)_2{\cdot}6H_2O$], copper nitrate [$Cu(NO_3)_2{\cdot}3H_2O$], zinc nitrate [$Zn(NO_3)_2{\cdot}6H_2O$], iron nitrate [$Fe(NO_3)_3{\cdot}9H_2O$], cerium nitrate [$Ce(NO_3)_3{\cdot}6H2O$] are taken in stoichiometric ratios and citric acid [$C_6H_8O_7{\cdot}H_2O$] is used a chelating agent. Mixed solutions of Metal nitrates and citric acid are evanesce in deionized water which concedes aqueous solution. It is mixed with 1:1 M ratio of nitrate to citric acid. The pH of mixed solution gets attuned to 7 using AR grade ammonia solution. The mixture is then neutralized with aqueous ammonia and heated upto 80 ^oC under constant stirring to transform into to gel form. When burst into flames at any point of the gel, the dried gel is burnt in a self-propagating combustion manner till all gel are wholly burnt out to form a fluffy loose ash auxiliary, it is further proceed in borosil glass beaker upon a hot plate for supplementary dry process. The ash is lightly ground and is calcined at 800 ^oC for 8 h so that the some impurity will evolve. Using X-ray diffraction (XRD), phase identification, crystalline size and lattice parameter have been characterized with Cu-Kα radiation. The crystalline size is calculated from peak broadening using Scherrer formula. Microstructure of the sintered specimens has been analyzed by scanning electron microscopy (SEM). Static magnetic properties like Saturation magnetization (M_s), remanent magnetization (M_r), coercivity (H_c), remanent ratio (M_r/M_s), etc, of the samples are measured at room temperature using vibration sample magnetometer (VSM), operating with magnetic field of 20 kOe. Polyvinyl acetate is used acts as a binder, the powder are uniaxially pushed to form palletes. The impedance analyzer is used to analyze dielectric properties, ac conductivity as well as dielectric loss factor.

III. RESULT AND DISCUSSION

3.1 XRD Analysis –

Figure 1 shows the X-ray diffraction patterns of sintered ferrites specimen ($Ni_{0.25}Cu_{0.2}Zn_{0.55}Fe_{2-x}Ce_xO_4$ with x=0.00, 0.05q, 0.1, 0.15, 0.2, 0.25) with varying Ce substitutions. The intense peaks in XRD of the specimens seem to suit with cubic spinel ferrite (JCPDS no. 08-0234). More conscientiously, the occurrence of intense diffraction peaks corresponding to the planes (111), (220), (311), (222), (400), (422), (511), (333), (440) confirms cubic spinel phase of the sample for x=0, but for x=0.05 to x=0.25 substitutions, in addition to Ni-Cu-Zn phase, CeO_2 phase is also present. This phase is detected in all Ce substituted samples. The peak intensity of CeO_2 slightly increases with Ce^{3+} concentration and indicates that the Ce^{3+}does not form the solid solution with spinel ferrite or it has small solid co-solubility with Ni-Cu-Zn [12-13]. XRD patterns for higher concentration of Ce^{3+} substituted Ni-Cu-Zn shows that intensity peak goes on decreasing which indicates the difficulty in the process of crystallization. George L *et al* [14] also find similar results when Ce is substituted with Ni-Zn mixed ferrite. Kabbur *et al* [15] shows that due to larger radii of rare earth ion as compared to Fe^{3+}, beyond a certain solubility limit, the secondary phase is introduced

because Fe^{3+} ions cannot be completely substituted by the rare earth ions. Hence, these ions gather around grain boundaries and form secondary phases.

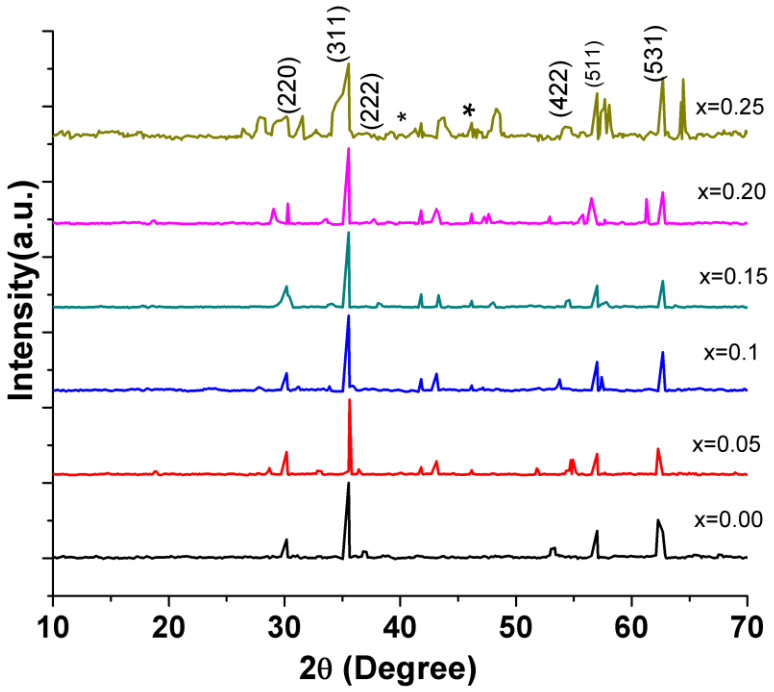

Figure 1. X-Ray diffraction Pattern for $Ni_{0.25}Cu_{0.2}Zn_{0.55}Fe_{2-x}Ce_xO_4$

The appropriate crystallographic parameters are calculated from X-ray diffraction peaks (hkl) using Scherer's formula and Bragg's relation. In the present case upto x=0.05, the crystallite size increases and beyond that limit for higher concentration of Ce^{3+}, it decreases as shown in table 1. The probable discernment for this is due to larger ionic radii of Ce^{3+} (1.02 Å) as compared to Fe^{3+} (0.64 Å). The difference in the ionic radii leads to the micro strain which consequently sets up domain wall motion resulting in deformation of the spinel structure. The lattice parameter (a) changes with x. It decreases with increase in the concentration of Ce, nevertheless, not monotonously. The decrease in lattice constant is supposed to the effect of occupancy of Ce^{3+} at tetrahedral sites which leads to contraction of unit cell. Similar results are observed by M. Kaiser *et al* [16] for rare earth substituted Ni-Zn-Cr.

Figure 2 reflects SEM (Scanning Electron Micrographs) images of $Ni_{0.25}Cu_{0.2}Zn_{0.55}Fe_{2-x}Ce_xO_4$ for x=0 to 0.25 (in steps of 0.05). It can be inferred from the SEM images that grain size of pure Ni-Cu-Zn ferrite with x=0.0 is larger than the doped samples of ferrite. The average grain size of pure Ni-Cu-Zn is found to be 0.92μm which then decreases with increasing Ce Concentration. The grain size varies from 0.92 μm to 0.24 μm. Presence of Ce^{3+} on the grain boundary instead of spinel lattice forming secondary phase CeO_2 causes hindrance in grain growth. Therefore, as the concentration of Cerium content rises in the ferrite, grain size of doped Ni-Cu-Zn decreases. The X-Ray density of the samples is obtained by the formula:

$D_x = 8M/N_A a^3$,

Where, M is the molecular weight of the sample, N is Avogadro's number and a^3 is the volume of the cubic unit cell. The X-Ray Density depends upon the molecular weight and lattice parameter of the sample. The bulk density (D_b) is obtained by

D_b= mass/πr^2,

Where, r be the radius and t be the thickness of sample pellets and the Porosity (P) percentage of the sample is given by relation $P = (1-D_b / D_x) *100$.

Figure 3 illustrates the variation of crystalline size (Å) with Ce content. Increase in X-Ray density of $Ni_{0.25}Cu_{0.2}Zn_{0.55}Fe_{2-x}CexO_4$ is found with increasing value of x. Large value of X-Ray density D_x as compared to D_b attributed to the subsistence of pores in the samples is in agreement with the large values of porosity for all samples. It is perceived that the porosity gets accelerated with Ce concentration.

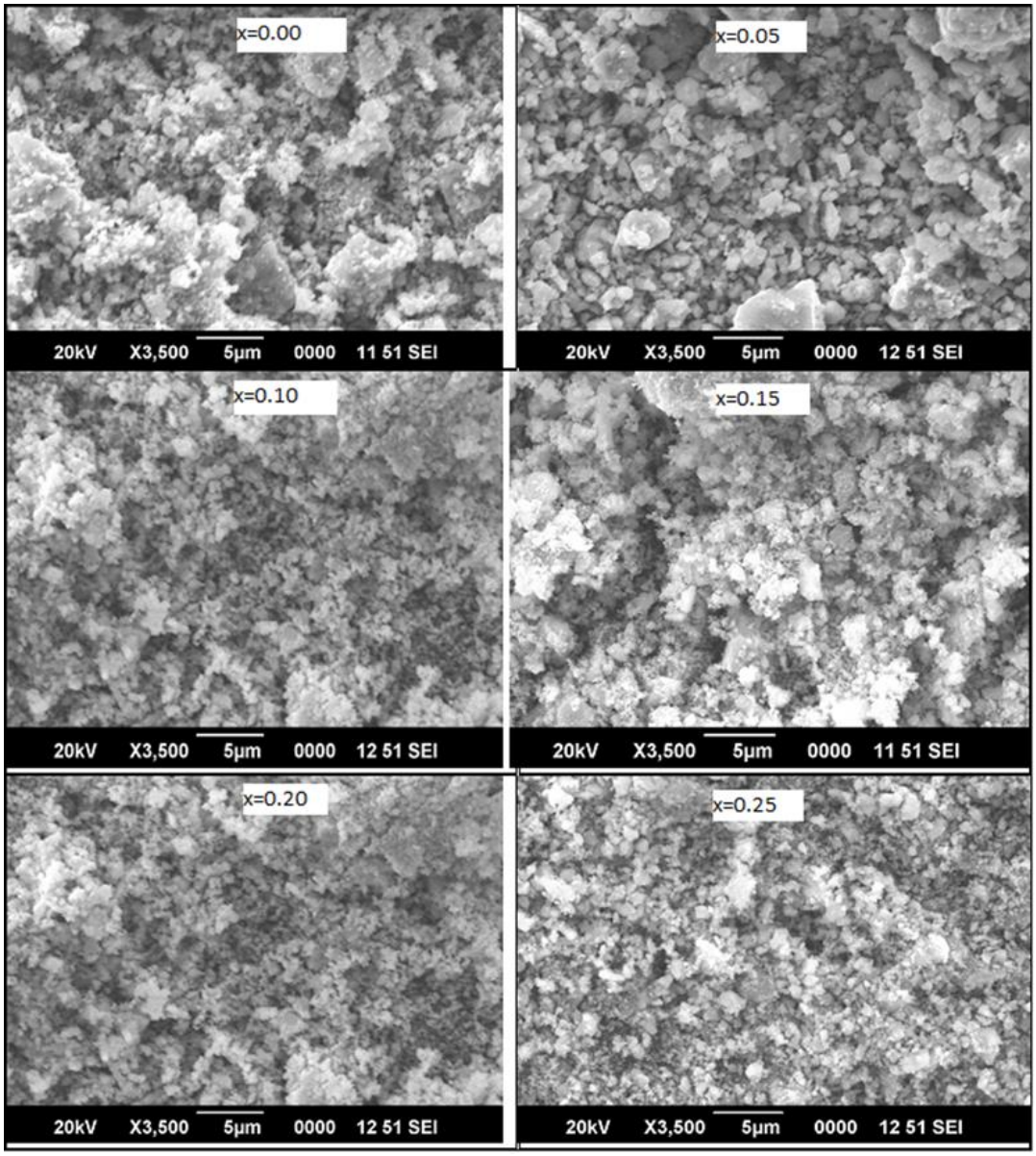

Figure 2. SEM images of $Ni_{0.25}Cu_{0.2}Zn_{0.55}Fe_{2-x}Ce_xO_4$

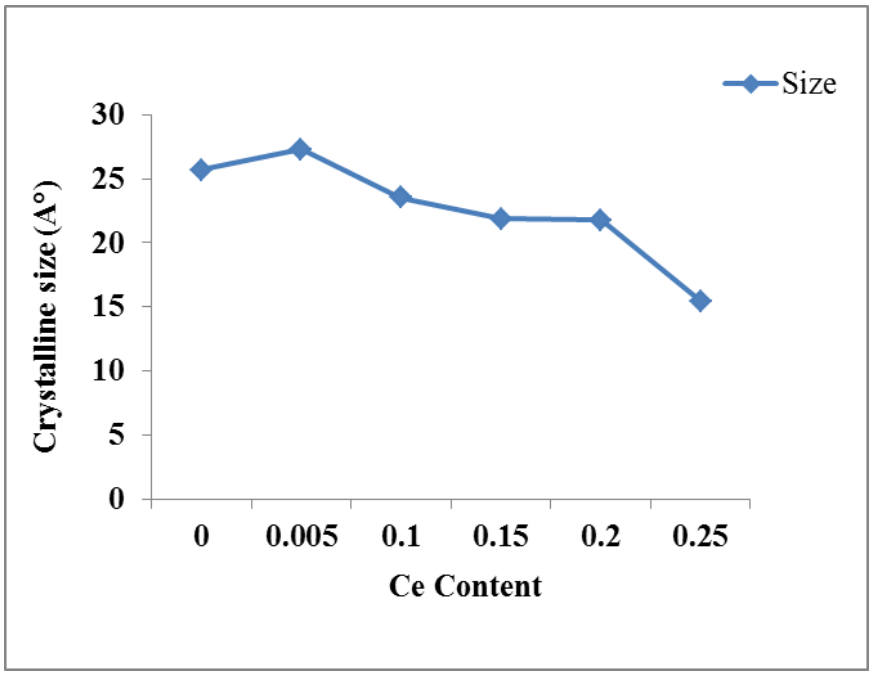

Figure 3. Variation of Crystaline size with Ce concentration

Table 1. Crystallite Size *(C)*, Lattice Constant *(a)*, X-Ray Density *(D_x)*, Bulk Density *(D_b)* Porosity *(P) and* Grain Size *(D)*

Content (x)	C (nm)	a (Å)	Dx (g/cm3)	Db (g/cm3)	P (%)	D (µm)
0	25.7021	8.487628	5.197211	2.32546	55.25561	0.92
0.005	27.3147	8.451083	5.216746	2.323178	55.25561	0.78
0.1	23.5214	8.49592	5.36195	2.2821	55.46692	0.26
0.15	21.8615	8.469121	5.505661	2.277536	57.43899	0.25
0.2	21.7997	8.432971	5.67014	2.508028	58.63283	0.24
0.25	15.4466	8.468922	5.690419	2.316332	55.76779	0.33

3.2 *VSM*

The magnetic measurements are carried out on the synthesized material from VSM analysis. M-H curve for samples of different concentration of Ce using VSM at room temperature is shown in Figure 4. The saturation magnetization (M_s), remanence (M_r), coercivity (H_c), remenant ratio (M_r/M_s), magnetic anisotropy of entire samples of $Ni_{0.25}Cu_{0.2}Zn_{0.55}Fe_{2-x}Ce_xO_4$ are tabulated in table 2.

It is found that M_s first increases with Ce content and it reaches to its maximum value of 55.09215 (emu/gm) at x=1.0 and then decreases. This kind of behavior is observed for remanant magnetization *(M_r)* and Magnetic anisotropy. The rise in magnetization is associated to the magnetic moment of the substituent ion.

It is implies the saturation magnetization (M_s) and remnant magnetization (M_r) is decreasing with the enhancement of Ce concentration. This decrease in magnetization (M_s) can be understood in terms of magnetic moment of Ce^{3+} ions. In the existingt case, octahedral B-sites occupied by Fe^{3+} ions are replaced by Ce^{3+} ions. But at room temperature, the magnetic dipole moment of rare earth ions is random and disordered and hence Ce^{3+} ions can be

considered as non-magnetic ions contributing zero magnetic moments. Thus, saturation magnetization decreases [17]. Also the replacement of rare earth ion to ferrite affects the A-B exchange interaction which determines the magnetization of rare earth doped ferrite. The occurrence of Ce at B-site weakens A-B exchange interfaces which also results in diminution of (M_s) [18].

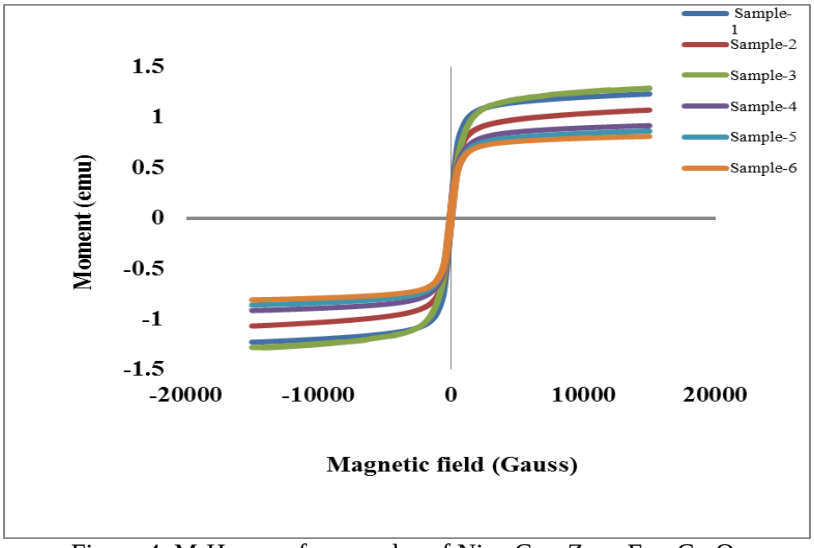

Figure 4. M-H curve for samples of $Ni_{0.25}Cu_{0.2}Zn_{0.55}Fe_{2-x}Ce_xO_4$

Table 1.Concentration*(x)*,Coercivity *(H_c)*,Remanence *(M_r)*,Magnetization *(M_s)*,Remanent Ratio (*M_r/M_s)*, Magnetic anisotropy *(K)*

Content (x)	H_c (G)	M_r (emu/gm)	M_s (emu/gm)	M_r/M_s	K
0	58.164	4.351714	58.50476	0.074382	3544.657
0.005	71.241	4.325864	48.59091	0.089026	3605.901
0.1	56.325	4.137783	55.92174	0.073992	4149.917
0.15	58.382	2.802391	39.78826	0.070433	2419.707
0.2	61.348	2.750348	37.45304	0.073435	3521.913
0.25	90.274	2.750348	35.18087	0.078177	3308.248

The remnant ratio (M_r/M_s) ia a handy evaluating unit and is the direction of magnetization gets oriented to the nearest magnetization direction subsequently the removal of magnetic field. Low value of (M_r/M_s) suggests isotropic nature of the material. It is observed that slight increase in remanent ratio with increasing Ce content. Magnetic anisotropy found to increase uniformly upto doping concentration x=0.1 but for high doping concentration it seems decreased with some uneven behavior. Above observations support the dependence of Magnetic properties of spinel ferrites on the grain size, cation substitution, A-B exchange interaction and magneto crystalline anisotropy.

Doping of Cerium causing significant modification in the coercivity of $Ni_{0.25}Cu_{0.2}Zn_{0.55}Fe_{2-x}Ce_xO_4$ samples. Large increase in coercivity happens for the bigger ionic radii of substituted Ce^{3+} ions as compared to Fe^{3+}. Some ions cannot enter the lattice but precipitate as secondary phase at the grain boundaries. The occurrence of impurities is precluding the grain evolution and hindering the motion of domain walls. This structural distortion may cause magnetic hardening of the material which resulting increase in coercivity of the ferrite [19].

3.3 Electrical Properties

Samples are used to compute the dielectric properties using impedance analyzer at room temperature. The real part of dielectric constant is enumerate with the assistance of the formula: $\varepsilon' = Cd/\varepsilon_0 A$, where, C is the capacitance of the pallet in farad, d is the thickness of the pallet in meter, The cross-segment area of the pallet and the permittivity in free space are A and ε_0.

The dielectric tangential loss factor is determined by utilizing the connection: $\tan \delta = 1/2\pi f RC$ where, δ is the loss angle, f is the frequency, R is the Resistance in pallet and C is the Capacitance. The imaginary dielectric constant ε'' has measured in terms of tangential loss factor ($\tan\delta$) as $.\varepsilon'' = \varepsilon' \tan \delta$ The AC conductivity is measured with the help of : $\sigma_{AC} = 2\pi f \varepsilon_0 \varepsilon' \tan\delta$.

3.3.1 Dielectric Properties

Figure 5 and figure 6 show the variation of real (έ) and complex part (ε") of dielectric constant with frequency for all the composition at room temperature. It is seen that the practices of real and imaginary part of dielectric constant are frequency based. These variations show that dielectric constant diminishes quickly in low frequency area and it is almost independent in higher frequency region. This behavior can also be clarified based on Koop's theory in accordance with Maxwell-Wagner two layer model in which ferrite materials ferrite materials should be considered. of exceptionally leading grains and they are isolated by ineffectively conducting grain limits [20]. Similar behavior were interpreted by other researchers [14-16]. The watched behavior in higher frequency region is because the electric dipoles can't pursue the fast variation of the alternating applied electric field at very high frequencies. Hence, the reluctance is offered to dipoles orientation and the alignment becomes slow [21]. The lower reaction of dielectric constant at higher frequency can be enlightened on the source of polarization. This dielectric distribution with frequency of material depends upon temperature, frequency of applied electric field, synthesis method and crystallite size. The presence of Fe^{3+} and Fe^{2+} ions at the octahedral B-sites give rise to dielectric polarization and rotational displacement of electric dipoles which result in the orientation of polarization. Interchange of Fe^{2+} and Fe^{3+} ions happens when electrons are bartered amongst the ions and the presence of Fe^{2+} and Fe^{3+} ions in the ferrite is liable for the space charge polarization and hopping mechanism between the localized state led to dielectric response [22].

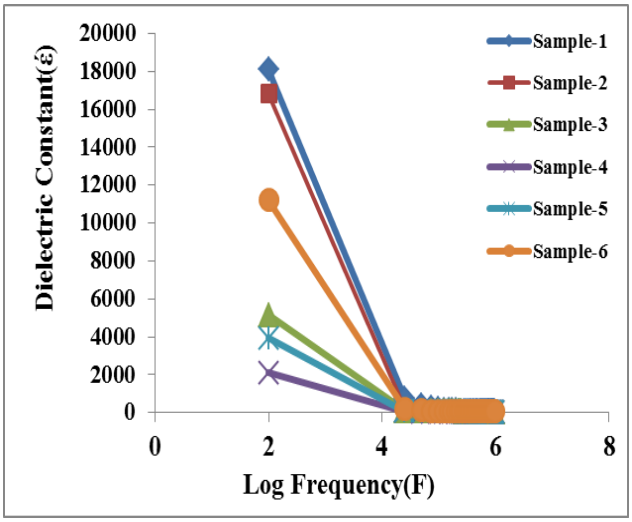

Figure 5. Variation of real part of dielectric constant (έ) with log(F)

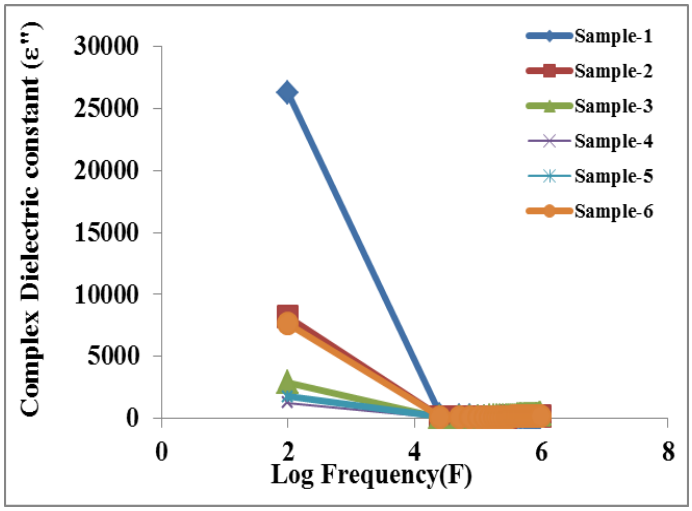

Figure 11. Variation of complex dielectric constant (ε") with log(F)

In the current case, it is additionally seen that the reduction in dielectric constant (έ) with escalation the concentration of Ce, the number of degree of freedom enriches. Analogous inferences are found by Sing and others [23-26]. Hence, the samples under consideration are more suitable for high frequency application.

3.3.2 Dielectric Loss

Figure 7 demonstrates at room temperature, the change in dielectric loss (tan δ) with frequency. Unlike most of the interpretations by others, the dielectric loss (tan δ) is increasing with increasing frequency. Dielectric loss may be due to the transfer of energy oscillator ions and hence power loss rises with the Ce concentration. Similar result is observed by R Srinivasa *et al* [26]. Dielectric loss depends on doping concentration of dopant.

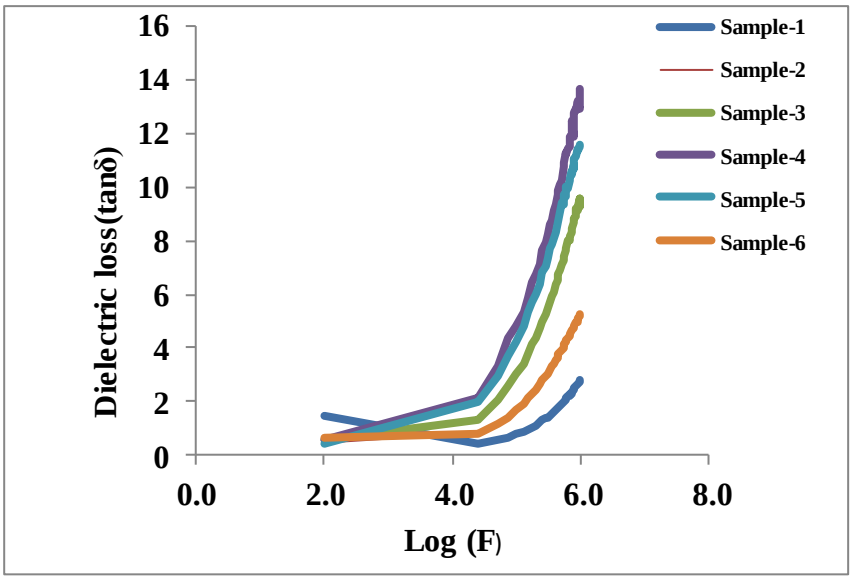

Figure 7. Variation of dielectric loss (tanδ) with log (F)

3.3.3 AC Conductivity

Figure 8 shows the compositional variational of AC Conductivity with frequency (log F) at room temperature. It seems that in higher frequency region with the proliferation in Ce concentration, AC conductivity increases. Complete conductivity of ferrite is caused by joined effect of dc conductivity and ac conductivity which are resulted from band and to hopping mechanism respectively. In this study, the AC conductivity stands unchanged in the low frequency region and increases snappishly in the altitudinous frequency zone which is universal dielectric behavior.

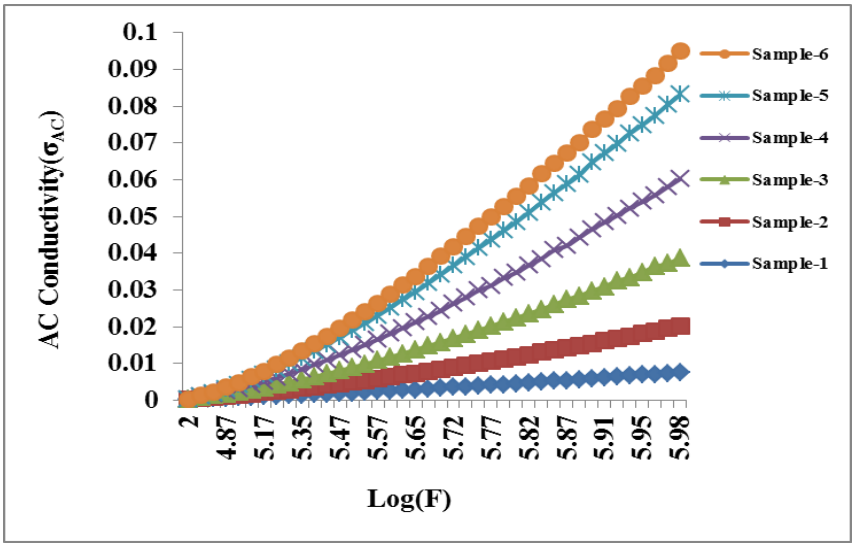

Figure 8. Variation of AC conductivity with log (F)

IV. CONCLUSION

In the existing study of $Ni_{0.25}Cu_{0.2}Zn_{0.55}Fe_2O_4$ spinel ferrite with general formulae $Ni_{0.25}Cu_{0.2}Zn_{0.55}Fe_{2-x}Ce_xO_4$ has been processed by sol gel method, XRD and SEM study corroborate the construction of cubic crystal system. The compound having zero content of ce is single phase and with doping of Ce secondery phase enhances. The crystalline size increases with Ce content upto and beyond that it decreases, the lattice parameter decreases with Ce but not monotonously. Porosity and X-ray density get escalated with Ce content. It is noticed from SEM images that grain size of pure sample is larger than doped sample. Saturation magnetization (M_s) and remanent magnetization (M_r) demonstrate an expanding pattern at first and the other way around with expanding dopant. Coercivity of dopant samples is proved to be higher than undoped sample. Low value of (M_r/M_s) suggests isotropic nature of the material. The dielectric constant is observed to be reliant of dependent on frequency. It diminishes quickly in low frequency region and almost independent in advanced frequency region. Dielectric loss depends on doping fixation. AC conductivity is almost constant in low frequency region and it increases speedily in high frequency region. The composition $Ni_{0.25}Cu_{0.2}Zn_{0.55}Fe_{1.85}Ce_{0.15}O_4$ demonstrates the better electromagnetic property among the all specimens and it is inferred as a better material for high frequency applications.

REFERENCES

[1] H. Harzali, F. Saida, A. Marzouki, A. Megriche, F. Baillon, F. Espitalier and A. Mgaidi, “Structural and magnetic properties of nano-sized NiCuZn ferrites synthesized by co-precipitation method with ultrasound irradiation”, J. Magn. Magn. Mater., Vol. 419, pp. 50-56, 2016.

[2] X. Wang, W. Qu, L. Li and Z. Gui, “The influence of Mn dopant on the electromagnetic properties of NiCuZn ferrite”, Ceram. Int., Vol. 30, No. 7, pp. 1615-1618, 2004.

[3] T. Nakamura, “Low-temperature sintering of NiZnCu ferrite and its permeability spectra”, J. Magn. Magn. Mater. , Vol. 168, No. 3, pp. 285-291, 1997.

[4] T. T. Ahmed, I. Z. Rahman and M. A. Rahman, “Study on the properties of the copper substituted NiZn ferrites”, J. Mater. Process. Techno, Vol. 153–154, pp. 797-803 2004.

[5] R. Lebourgeois, S. Duguey, J. .P Ganne and J. M. Heintz, “Influence of V_2O_5 on the magnetic properties of nickel–zinc–copper ferrites”, J. Magn. Magn. Mater., Vol. 312, No. 2, pp. 328- 330, 2007.

[6] H. Su, H. Zhang, X. Tang and X. Xiang, “High permeability and high Curie Temperature Ni-Cu-Zn ferrite”,J. Magn. Magn. Mater., Vol. 283, pp. 157- 163, 2004.

[7] B. Li, Z. Yue, X. Wei Qi, J. Zhou, Z. Lun Gui and L. Li, Mater. Sci. Eng.,Vol. 99, No. 1-3, pp. 252-254, 2003.

[8] H. Su, H. Zhang, X. Tang and Y. Shi, “Effects of microstructure on permeability and power loss characteristics of the NiZn ferrites” J. Magn. Magn. Mater. Vol. 320,No. 3-4, pp. 483-485, 2008.

[9] S. R. Murthy, “Low temperature sintering of NiCuZn ferrite and its electrical, magnetic and elastic properties”, J. Mater. Sci. Lett. Vol. 21,No. 8, pp. 657-660, 2002.

[10] M. Fujimoto, “Inner Stress Induced by Cu Metal Precipitation at Grain Boundaries in Low-Temperature-Fired Ni-Zn-Cu Ferrite”, J. Am. Ceram. Soc., Vol. 77, No. 11, pp. 2873-2878, 1994.

[11] Y. Xun Li, J. Li,Quiang Li, G. Liang Yu, H. Wu Zhang,” Structure and magnetic properties of NiCuZn ferrite materials with La doping”,Rare metals, Vol. 36, No.3,pp. 202-204,2017.

[12] P. K. Roy, J. Bera,”Electromagnetic properties of samarium-substituted NiCuZn ferrite prepared by auto-combustion method”, J. Magn,. Magn. Mater., Vol. 321, No. 4, pp. 247-251, 2009.

[13] L. Qing, L. Chenglong, H. Yun, X. Jianmei,W. Ruijun,”Mössbauer and XRD Studies of $N_{0.6}Cu_{0.2}Zn_{0.2}Ce_x Fe_{2-x}O_4$ Ferrites by Sol–Gel Auto-Combustion”,Journal of Nanoscience and Nanotechnology,Vol. 15,No.4,pp.2997-3003,2015.

[14] L. George, C. Viji, H. Mathew, E. M. Mohammed, “Structural, Dielectric, Magnetic and Optical Properties of Cerium Substituted Ni-Zn Mixed Ferrite”,Material Sci. Res. India., Vol. 14, No. 2, pp. 133-139, 2017

[15] S. M. Kabbur, S. D. Waghmare, D. Y. Nadargi, S. D. Sartale, R. C. Kambale, U. R. Ghodake, S. S. Suryavanshi, “Magnetic interactions and electrical properties of Tb3+ substituted NiCuZn ferrites”, Journal of Magnetism and Magnetic Materials, Vol. 473, pp. 99-108 2019.

[16] M. Kaiser, “Effect of rare earth elements on the structural, magnetic and electrical behavior of Ni-Zn-Cr nanoferrites”, Journal of Alloys and Compounds, Vol. 719, pp. 446-454, 2017.

[17] S. I. Ahmad, S. I. Kumar, D. R. Syed, et al, Structural, Spectroscopic and Magnetic Study of Nanocrystalline Cerium-Substituted Magnesium Ferrites, Arab J Sci. Eng, Vol. 42, No. 1, pp. 389-398, 2017.
[18] M. F. Huq, D. K. Saha, R. Ahmed, Z. H. Mahmood, "Ni-Cu-Zn Ferrite Research: A Brief Review", Journal of Scientific Research, Vol. 5, No. 2,pp. 215-234 , 2013.
[19] X. C. Zhong, X. J. Guo, S. Y. Zou, H. Y. Yu, Z. W. Liu, Y. F. Zhang, and K. X. Wang, "Improving soft magnetic properties of Mn-Zn ferrite by rare earth ions doping", AIP Advances, Vol. 8, No. 4, pp. 047807 , 2018.
[20] C. G. Koops, "On the Dispersion of Resistivity and Dielectric Constant of Some Semiconductors at Audio frequencies", Phys. Rev., Vol. 83, pp.121, 1951.
[21] N. Sivakumar, A. Narayanasamy, B. Jeyadevan, R. J. Joseyphus, C .Venkateswaran, "Dielectric relaxation behavior of nanostructured Mn–Znferrite"J.Phys.DAppl.Phys.,Vol. 41,No.24,pp.245001-249901,2008.
[22] R. Rani, G. Kumar, K. M. Batoo, M. Singh, "Influence of temperature on the electric,dielectric and AC conductivity properties of nano-crystalline zinc substituted cobalt ferrite synthesized by solution combustion technique", Appl. Phys. A, Vol. 115, No.4, pp. 1401-1407, 2014.
[23] R. K. Singh, J. Shah, R. K. Kotnala, "Magnetic and dielectric properties of rare earth substituted $Ni_{0.5}Zn_{0.5}Fe_{1.95}R_{0.05}O_4$ (R = Pr, Sm and La) ferrite nanoparticles", J. Mater. Sci. Eng. B, vol. 210, pp. 64-69, 2016.
[24] M. F. Din, G. Murtuza, I. Ahmad, M. F. Warsi, "Magnetic, ferromagnetic resonance and electrical transport study of $Ni_{1-x}TbxFe_2O_4$ spinel ferrites", Ceramics International, Vol. 40,No.2, pp. 3571-3577, 2014.
[25] B. P. Jacob, S Thankachan, S. Xavier, E. M. Mohammed, "Dielectric behavior and AC conductivity of Tb^{3+} doped $Ni_{0.4}Zn_{0.6}Fe_2O_4$ nanoparticles", Journal of Alloys and Compounds, Vol. 541, pp. 29-35, 2012.
[26] P. V. S. Rao, T. Anjaneyulu, D.V. Krishna Reddy, M. Rami Reddy, "Magnetic and Electrical Properties of Gd Doped Ni-Cu-Zn-Fe_2O_4", Advances in Materials Physics and Chemistry, Vol. 8,pp. 401-410, 2018.